Power Electronic Systems
Laboratory

Proceedings of the International Power Electronics Conference - ECCE Asia (IPEC 2014), Hiroshima, Japan, May 18-21, 2014

Novel Principle for Flux Sensing in the Application of a DC + AC Current Sensor

L. Schrittwieser,
M. Mauerer,
D. Bortis,
G. Ortiz,
J. W. Kolar

Eidgenössische Technische Hochschule Zürich
Swiss Federal Institute of Technology Zurich

Novel Principle for Flux Sensing in the Application of a DC + AC Current Sensor

L. Schrittwieser*, M. Mauerer*, D. Bortis*†, G. Ortiz*† and J. W. Kolar*
*Power Electronic Systems Laboratory, ETH Zurich, Switzerland
†Enertronics GmbH, Switzerland
Email: bortis@lem.ee.ethz.ch

***Abstract*—Magnetostriction describes the geometrical change in length of a ferromagnetic material in dependence of its internal magnetic flux density value. By detecting the vibrations caused by these dimensional changes with a piezo-electric transducer, the instantaneous value of the magnetic flux inside a magnetic core can be sensed from DC up to a few kilohertz. This principle, together with a high bandwidth current transformer, was utilized in order to construct a current sensor capable of measuring currents ranging from DC to several MHz. As will be shown in this paper, an additional sinusoidal AC-excitation of the core material provides higher sensitivity of the length measurement and overcomes the high-pass characteristic of the piezo sensor. In order to prove the principle and to demonstrate the capabilities of this new sensor, a series of experimental measurements and implementation results are presented.**

I. INTRODUCTION

Precise current measurement is a mandatory requirement of modern power electronic systems as it enables the implementation of high performance current control loops, monitoring and safe shut-down in case the maximum allowed current value has been exceeded, among others.

Depending on the specific application and the required performance of the measurement system, the existing current measurement concepts can be classified according to their key operating principles. **Fig. 1** gives an overview of the most common current measurement methods that are applicable in power electronics whereby their key features are presented in the following.

A. Isolated Current Measurement Concepts

If a galvanic isolation between the current to be measured and the sensor is required, the measurement principle is typically based on *Ampère's Law* where effects caused by the magnetic field of the current are exploited. There, Rogowski coils or AC current transformers are commonly used when only AC currents need to be measured, e.g. in power transmission systems [1][2].

On the other hand, if AC as well as DC current components need to be captured, several techniques are applicable. Magneto-resistive sensors make use of the fact that some materials change their resistance in the presence of a magnetic field [3]. Magneto-optical current sensors exploit the *Faraday Effect* and are usually applied in high-current applications [4]. There are many methods involving a saturable magnetic material in order to measure current. Sensors of this kind can be operated in open or closed loop systems and usually require more than one magnetic core [5]. Current can also be measured by introducing a semiconductor Hall-effect sensor in the magnetic path in order to directly measure the magnetic field caused by the current. These current sensors can be operated in open or closed loop configurations as well and they can be combined with a current transformer to achieve a higher bandwidth [6].

B. Non-isolated Current Measurement Concepts

If no galvanic isolation is required, the current can be measured by using *Ohm's Law* and a shunt resistor [6]. In order to achieve a high bandwidth of several tens of megahertz or more, special construction techniques for the shunt are required in order to reduce parasitic effects [7].

C. Proposed Concept

The new current measurement technique is based on the magnetostriction effect. Other sensors based on inverse magnetostriction have been presented [8]. However, the new sensor directly measures the change in length of a magnetic core to gain information about its magnetic flux density. This information is then used together with a current transformer in order to accurately measure both static and time-varying current components.

Compared to a current probe that utilizes a hall sensor, this system does not require any interruption of the magnetic path in order to introduce the flux sensor. The operation principle and the theoretical background of this new technology are presented in the following.

II. THEORY OF OPERATION

The proposed current sensor is based on a current transformer which provides a galvanic isolation as described in the previous section. Since current transformers have a high-pass characteristic given by their magnetizing inductance and the burden resistance, no DC currents can be measured.

As described in [9] and [10], in order to be able to measure also the low frequency components of the current, often a closed-loop flux compensation circuit consisting of a flux sensor (e.g. a Hall effect sensor inserted into the air gap of the magnetic core), an op-amp circuit and a compensation winding is added. The current through the compensation winding is controlled in such a way that an operation of the magnetic core at zero flux density can be ensured (cf. **Fig. 2 a)**). This way, the current in the compensation winding is proportional (depending on the measurement to compensation winding's turns ratio) to the input current i_{in}.

With this configuration, frequency components above the current transformer's lower cut-off frequency ($i_{\mathrm{in,HF}}(t)$)

978-1-4799-2705-0/14/$31.00 ©2014 IEEE

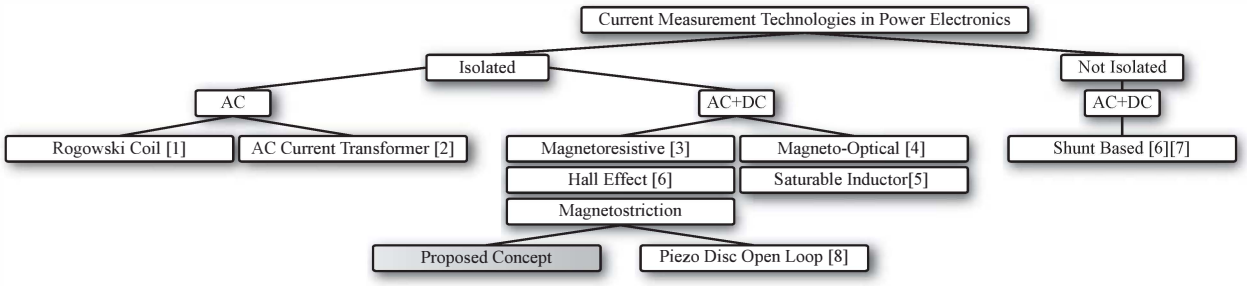

Fig. 1: Overview of previously presented current measurement technologies utilized in power electronic systems.

would cause a magnetic flux $B_{\mathrm{in,HF}}(t)$ in the core, which is compensated by the high frequency current $i_{\mathrm{m,HF}}(t)$ flowing in the measuring winding and through the burden resistor R_{B}. Due to the core material's high permeability, the resulting magnetizing flux is very small at these frequencies, thus no signal will be measured by the flux sensor. On the other hand, any frequency components which are below the current transformer's lower cut-off frequency ($i_{\mathrm{in,LF}}(t)$) would not induce a voltage in the burden winding. However, they are captured by the flux sensor and therefore will be compensated by the current $i_{\mathrm{m,LF}}(t)$ in the compensation winding, allowing a measurement with bandwith ranging from DC to several MHz.

It has to be emphasized that for this configuration, no frequency response matching of the flux sensor and the current transformer is necessary. However, in order to be able to compensate this low frequency flux, the current transformer's lower cut-off frequency has to be well below the flux sensor's upper cut-off frequency. Then, the measurement error caused by the magnetizing inductance of the transformer is negligible.

Instead of using an additional compensation winding, the compensation current can also be fed directly into the measurement winding as shown in **Fig. 2 b)**. Both, the low frequency compensation current and the current transformed to the measurement winding, are then forced through the same winding, thus also through the burden resistor R_{B}. Consequently, both current components $i_{\mathrm{m,LF}}(t)$ and $i_{\mathrm{m,HF}}(t)$ are inherently added and the voltage across the burden resistor R_{B} is directly proportional to the current $i_{\mathrm{in}}(t)$ [9].

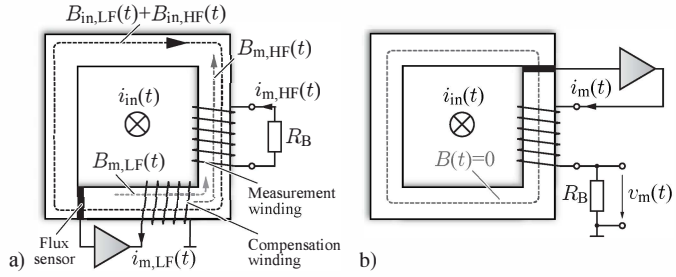

Fig. 2: Flux compensated current transducer concept: **a)** A flux sensor is inserted in the magnetic path and its signal is used to compensate the low frequency components of the main current. The high frequency components are measured by a current transformer. **b)** Integrated flux measurement and current transformer.

A. Magnetostriction-based Flux Sensing

The flux sensor, typically a hall-element, is the crucial part of an actively compensated current transformer design since its signal allows the controller to close the loop. Another possible way to sense the magnetic flux is to use the magnetostriction phenomenon, as proposed in this paper.

Basically, magnetostriction is the relative change in length $\Delta l/l$ of a magnetic material when a magnetic flux density B is applied. As described in [11] and [12], the change of length is proportional to the square of the magnetic flux density for flux densities much smaller than the saturation flux density B_{S}. The common magnitude for this effect is typically given as saturation magnetostriction λ_{S} which describes the relative change in length reached at saturation flux density (cf. (1)).

$$\frac{\Delta l}{l}(B) \approx B^2 \cdot \frac{\lambda_{\mathrm{S}}}{B_{\mathrm{S}}^2} \qquad \text{for} \quad B \ll B_{\mathrm{S}}. \tag{1}$$

The magnetostriction can be measured e.g. with an electromechanical transducer which converts the change in length into an electrical output voltage. Possible electromechanical transducers are strain gauges or piezo elements. A strain gauge changes its electric resistance depending on the applied elongation, thus constant elongations can be captured. Piezoelectric transducers, on the other hand, feature an inherent high pass characteristic. Consequently, only elongations above its lower cut-off frequency can be measured. Piezoelectric sensors are available with a higher sensitivity than strain gauges. As a consequence, a piezo sensor was used for the implementation of the prototype.

Due to the dependency on B^2 in (1), a direct measurement of the transformer core's change in length $\Delta l/l$ results in a non-linear sensor output signal $v_{\mathrm{s}}(t)$. In addition, the sign of the flux and therefore the sign of the magnetization current, is not preserved. Thus, even if the quadratic relationship between the flux and the change in length could be linearised, the requirement of the flux's sign would make it impossible to control the magnetic flux to zero without additional precautions taken.

The aforementioned drawbacks can be overcome by injecting an AC voltage signal through an additional winding in the current sensor's magnetic core, as shown in **Fig. 4**) and as will be discussed in the following.

B. AC Excitation

An additional winding N_{ex}, connected to a sinusoidal voltage source v_{AC}, is added to the core in order to create a new sinusoidal component $B_{\mathrm{ex}}(t) = \widehat{B}_{\mathrm{ex}} \sin(\omega_{\mathrm{ex}} t)$ in the core flux (cf. **Fig. 4**).

Since the frequency components above the current transformer's lower cut-off frequency $B_{\mathrm{HF}}(t)$ are already compensated by the measuring winding, the flux measured by the flux sensor is $B(t) = B_{\mathrm{LF}}(t) + \widehat{B}_{\mathrm{ex}} \sin(\omega_{\mathrm{ex}} t)$. In **Fig. 3 a)** the resulting spectrum of the flux $B(t)$, with an upper cutoff frequency of ω_{LF}, is shown. Based on (1) and the given spectrum of the flux $B(t)$, the spectrum of the flux sensor's output signal $v_{\mathrm{s}}(t)$ can be calculated as

$$\begin{aligned} v_{\mathrm{s}}(t) \propto B^2(t) &= \left(B_{\mathrm{LF}}(t) + \widehat{B}_{\mathrm{ex}} \sin(\omega_{\mathrm{ex}} t)\right)^2 \\ &= B_{\mathrm{LF}}^2(t) + \frac{\widehat{B}_{\mathrm{ex}}^2}{2} + \underbrace{2 B_{\mathrm{LF}}(t) \widehat{B}_{\mathrm{ex}} \sin(\omega_{\mathrm{ex}} t)}_{\text{AM Modulated Excitation}} \\ &\quad + \frac{\widehat{B}_{\mathrm{ex}}^2}{2} \sin(2\omega_{\mathrm{ex}} t) \end{aligned} \tag{2}$$

and is illustrated in **Fig. 3 b)**. As can be noticed from (2) and **Fig. 3 b)**, with the superposition of the excitation flux $B_{\mathrm{ex}}(t)$ and the low frequency flux $B_{\mathrm{LF}}(t)$, new frequency components are introduced. The spectrum of the sensor voltage differs from the spectrum of the core flux density in several aspects; a new component occurs at twice the excitation frequency $2\omega_{\mathrm{ex}}$ due to the squaring of the excitation signal $B_{\mathrm{ex}}(t)$. Furthermore, the low frequency signal's amplitude is squared and the bandwidth is doubled to $2\omega_{\mathrm{LF}}$. In addition, the DC-value is increased by $\widehat{B}_{\mathrm{ex}}^2/2$. The most important difference, however, is the fact that the excitation frequency component gets modulated by the original low frequency spectrum of $B_{\mathrm{LF}}(t)$. This means that the spectrum of $B_{\mathrm{LF}}(t)$ is now centered around the excitation frequency ω_{ex} (cf. middle term in (2) and **Fig. 3 b)**) which is in accordance with measurements published in [13].

For this reason, the modulated signal which is now purely AC, can easily be measured with a piezoelectric transducer, whereby the transducer's lower cut-off frequency has to be below $\omega_{\mathrm{ex}} - \omega_{\mathrm{LF}}$. In addition, based on **Fig. 3 b)**, it can be noticed that the excitation frequency ω_{ex} has to be at least three times higher than the lower cut-off frequency of the transformer ω_{LF}. Otherwise, the spectrum centered around the excitation frequency ω_{ex} would overlap with the spectrum of $B_{\mathrm{LF}}^2(t)$ which would result in a distortion of the original signal $B_{\mathrm{LF}}(t)$. In this case, the modulated signal can be used to measure the low frequency signal $B_{\mathrm{LF}}(t)$. Hence, the desired spectrum centered around the excitation frequency ω_{ex} has to be isolated by the use of a suitable bandpass filter (cf. **Fig. 4**). The spectrum of the filtered output signal $v_{\mathrm{BP}}(t)$ is shown in **Fig. 3 c)**.

In a further step, the bandpass filtered signal $v_{\mathrm{BP}}(t) \propto \widehat{B}_{\mathrm{ex}} \sin(\omega_{\mathrm{ex}} t)$, whose amplitude depends linearly on $B_{\mathrm{LF}}(t)$, can be demodulated by the multiplication with $\sin(\omega_{\mathrm{ex}} t)/\widehat{B}_{\mathrm{ex}}$. This yields the demodulator output $v_{\mathrm{D}}(t)$ containing the intended component $B_{\mathrm{LF}}(t)$ as well as a copy

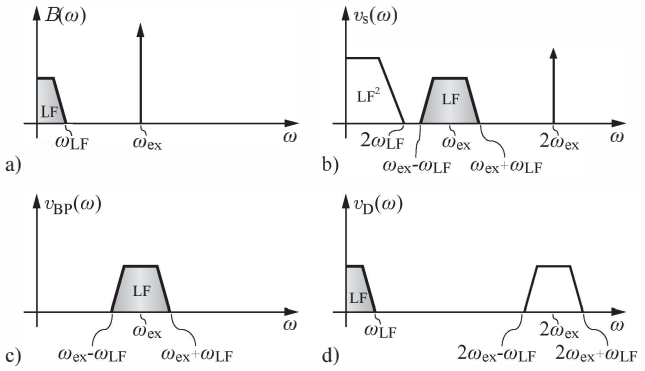

Fig. 3: Resulting spectra with AC-excitation, spectrum of **a)** the magnetic flux, **b)** the flux sensor's output signal, **c)** the bandpass filtered signal and **d)** the demodulated signal.

of this spectrum centered around $2\omega_{\mathrm{ex}}$ as shown in **Fig. 3 d)**. With a subsequent low pass filter, this copy can be discarded.

This principle allows the sensing of positive as well as negative magnetization currents without applying an additional offset current. Furthermore, the amplitude $\widehat{B}_{ex}$ of the excitation signal gives a degree of freedom which allows to scale the magnetostriction signal amplitude independently of the magnitude of $B_{LF}(t)$. Also, no DC signal has to be measured by the magnetostriction sensor. This allows the usage of piezo transducers which have an inherent high pass characteristic and it eliminates problems with DC drifts and offsets of amplifiers in the signal path. However, the AC excitation flux in the core will induce a voltage in the measurement winding and will therefore disturb the measured signal. This has to be compensated by using a second transformer as it will be explained in the following.

C. Compensation Transformer

Since the AC-excitation signal is also transformed to the other windings, i.e. the burden winding as well as the conductor whose current has to be measured, a second transformer T_2 with the same winding arrangement as for transformer T_1 is connected in series to T_1, with the only difference that the orientation of the excitation winding is reversed (cf. **Fig. 5**). Consequently, in both cores of T_1 and T_2, the same AC-excitation signal with opposite sign is impressed, which - assuming identical properties of the two transformers - is cancelled out in the other windings. However, due to production and assembly tolerances prevalent in a real system, the two transformers will not be

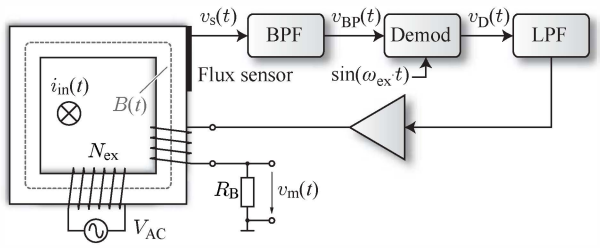

Fig. 4: Block diagram of AC-excitation and signal processing of the magnetostriction-based flux sensor.

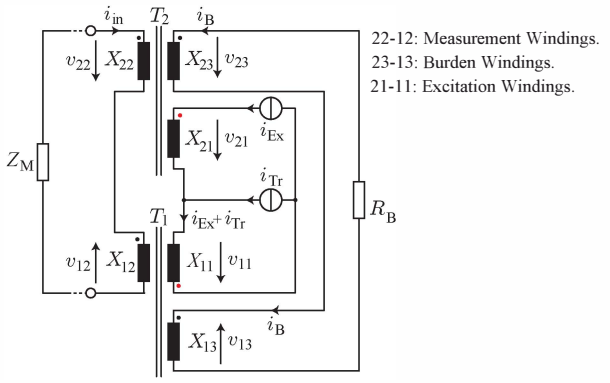

Fig. 5: Schematic representation of the current transducer comprising measurement windings, burden windings and excitation windings. These last ones are used in order to inject the AC high frequency signal and to perform the required trimming in the magnetic core.

exactly identical. This leads to an incomplete cancellation of the excitation signal in both the burden winding and in the measured conductor. This problem can be minimized by introducing an additional current source $i_{\mathrm{Tr}}(t)$ at the connection point of the two excitation windings (cf. **Fig. 5**). The following section will reveal that with this additional current source, the undesired effects introduced by the non-identical transformers can be significantly reduced.

D. Trimming

As mentioned above, the current source $i_{\mathrm{Tr}}(t)$ in **Fig. 5** can be used to trim the system in such a way that undesired signals, introduced by the slightly different transformers, can be eliminated. The aim of this investigation is to analyze the effects introduced by the excitation current on the current in the burden winding i_{B} as well as the current in the measurement winding i_{in}. In order to investigate the possibilities and limitations of this approach, some simplifications are made. The excitation voltage source is replaced with a current source $i_{\mathrm{Ex}}(t)$. Furthermore, the compensation voltage source in the burden winding path is omitted since it operates independently from the excitation and trimming system. It is also assumed that an arbitrary impedance Z_{m} is connected to the measurement winding. This is the impedance of the circuit providing the current i_{in} which is measured. Voltage sources in series with Z_{m} and current sources in parallel with it do not affect the trimming system and hence are omitted. Additionally, the transformers are assumed to be linear.

Both transformers have three windings, denoted as follows: Winding 1 is the excitation winding, winding 2 is the measurement winding and winding 3 is the burden winding. With reference to **Fig. 5**, T_2, a three-winding transformer can be described, for AC steady state analysis, in the following way:

$$\begin{bmatrix} \underline{v}_{21} \\ \underline{v}_{22} \\ \underline{v}_{23} \end{bmatrix} = \begin{bmatrix} \underline{X}_{21} & \underline{X}_{21\_2} & \underline{X}_{21\_3} \\ \underline{X}_{22\_1} & \underline{X}_{22} & \underline{X}_{22\_3} \\ \underline{X}_{23\_1} & \underline{X}_{23\_2} & \underline{X}_{23} \end{bmatrix} \cdot \begin{bmatrix} \underline{i}_{\mathrm{Ex}} \\ \underline{i}_{\mathrm{M}} \\ \underline{i}_{\mathrm{B}} \end{bmatrix},$$

whereby:

$$\underline{X}_{\mathrm{xyz}} = j\omega \cdot L_{\mathrm{xyz}}.$$

L_{21}, L_{22} and L_{23} are the self inductances of winding 1, 2 and 3 respectively. L_{21_2} is the mutual inductance between winding 1 and 2. Note that the inductance matrix is symmetric, e.g. $L_{21\_2} = L_{22\_1}$.

Using these equations, the circuit in **Fig. 5** can be analyzed to determine the currents in the burden and measurement windings caused by the excitation and trimming currents. The result is shown in equations (3) and (4).

$$\underline{i}_{\mathrm{B}} = \frac{\underline{i}_{\mathrm{Ex}}(\underline{X}_{13\_1}-\underline{X}_{23\_1})-\underline{i}_{\mathrm{M}}(\underline{X}_{13\_2}+\underline{X}_{23\_2})+\underline{i}_{\mathrm{Tr}}\cdot\underline{X}_{13\_1}}{R_{\mathrm{B}}+\underline{X}_{13}+\underline{X}_{23}} \quad (3)$$

$$\underline{i}_{\mathrm{in}} = \frac{\underline{i}_{\mathrm{Ex}}(\underline{X}_{12\_1}-\underline{X}_{22\_1})-\underline{i}_{\mathrm{B}}(\underline{X}_{12\_3}+\underline{X}_{22\_3})+\underline{i}_{\mathrm{Tr}}\cdot\underline{X}_{12\_1}}{\underline{Z}_{\mathrm{M}}+\underline{X}_{12}+\underline{X}_{22}} \quad (4)$$

Both equations reveal that the disturbance, caused by the excitation current, depends on the difference of the transformer's mutual inductances. This holds for both currents, in the burden winding as well as in the measurement winding. It can be seen that, if the transformers have identical mutual inductances, no disturbance will be caused by the excitation current.

Assuming non-identical transformers, the trimming current $\underline{i}_{\mathrm{Tr}}$ allows the elimination of the coupled excitation signal in either the measurement or the burden winding, but not in both. This is due to the fact that the measurement and burden windings in the two transformers do not necessarily show the same difference in mutual inductances with respect to the excitation windings and there is only one degree of freedom, the trimming current $\underline{i}_{\mathrm{Tr}}$. Hence the excitation signal can only be cancelled in one winding. The goal is to eliminate the excitation signal in the burden winding since the current in the burden winding represents the output signal of the system and is directly measured. Hence it can be used as an input for the trimming system. The prototype system has shown that the remaining disturbance in the measurement winding, due to the asymmetry of the transformers, can be neglected even for small $\underline{Z}_{\mathrm{M}}$ since it is possible to produce two very similar transformers.

Combining equations (3) and (4) yields a rather complex expression for $\underline{i}_{\mathrm{B}}$. However, as $\underline{i}_{\mathrm{B}}$ depends linearly on $\underline{i}_{\mathrm{Tr}}$, there exists a unique solution to the equation $\underline{i}_{\mathrm{B}} = 0$. Therefore, the trimming system allows to drive the current in the burden winding to zero, eliminating any coupled excitation currents.

Since there are many parameters involved in this system, a calculation of the necessary trimming current is complex. The prototype of the current probe therefore uses a search algorithm to determine the required phase and amplitude of the trimming current in order to reduce the disturbing burden current to a minimum. The algorithm works by applying several equally spaced current phase angles with constant amplitude. In the first sweep, the tested phase angles span over the full parameter range, i.e. $[0, 2\pi]$. For each point, the amplitude of the excitation frequency component is measured using a matched filter. Once all points have been measured, the phase angle resulting in the lowest distortion, is selected. The next sweep will cover only a part of the parameter space in order to narrow down the search. As the parameter space

is two dimensional, the same sweeping technique is applied to the amplitude of the trimming signal.

III. Implementation Results

In order to verify the new current measurement principle, a compact prototype has been built. It is capable of measuring currents up to $\pm 20\,\mathrm{A}$ with a bandwidth of DC to $20\,\mathrm{MHz}$. As described above, two magnetic cores, showing a relatively high magnetostriction, are the key components.

Fig. 6 depicts the core setup of the prototype. In the picture, the second transformer core is behind the first core. The two cores are connected to the circuitry depicted in **Fig. 7** which performs all the required signal processing.

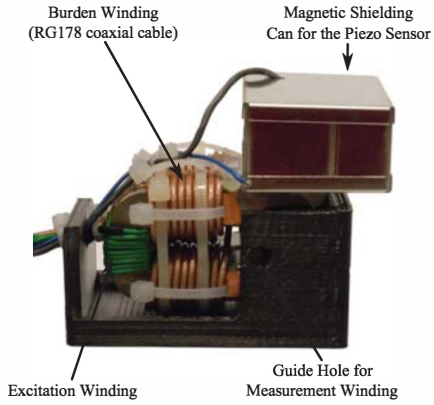

Fig. 6: Current transducer components' arrangement.

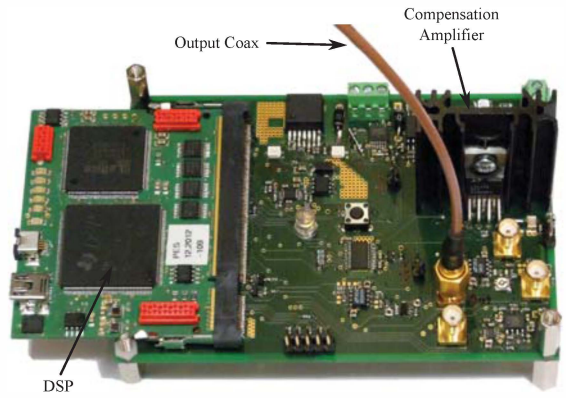

Fig. 7: Analog and digital circuits utilized for signal processing.

A. Transformer Core

For the two transformers, *AMCC-4* C-shaped cores made from the amorphous material *2605SA1* from *Hitachi Metals/Metglas* were used. This material was selected as it shows the highest magnetostriction of the tested materials. Furthermore, cores of this material suitable to build a current transformer with are available. **Fig. 8** illustrates the arrangement of such a transformer. For the burden winding, an *RG178* coaxial cable was used in order to shield the burden winding from external electric fields. The current transformer itself, without flux compensation, has lower cut-off frequency of $\approx 530\,\mathrm{Hz}$. **Table I** lists the measured properties of the

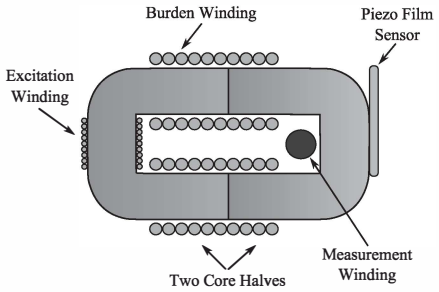

Fig. 8: Winding arrangement of one of the transformers and the respective piezo transducer.

two transformer cores. Note that k is the coupling factor between the windings. The well known relationship between the mutual inductance and the coupling factor is as follows:

$$k = \frac{L_{21\_2}}{\sqrt{L_{21} L_{22}}} \tag{5}$$

An ideal transformer has coupling factors of 1. The coupling factors involving the measurement winding depend on the position of the measurement winding within the transformer as well as its length. As long as the winding arrangement is similar for both transformers, the coupling factors are almost identical as well and as a consequence, so are the mutual inductances.

B. Piezo Film Sensor

In order to measure the core's magnetostriction, an electrically shielded *SDT1-028k* piezo film sensor from *Measurement Specialities* is adhered to one of the two magnetic cores. The sensor, as depicted in **Fig. 9**, is approximately 30 mm long. Its terminals and cable are electrically shielded, as is the sensor element itself. This reduces electrical interference to the sensor output. However, the sensor is not shielded against magnetic fields. As a consequence, care must be taken in order to avoid the generation of faulty sensor output singals due to stray magnetic fields. In the prototype, the sensor was rigidly placed inside a magnetic shielding can.

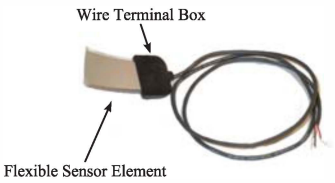

Fig. 9: *SDT1-028k* piezo film sensor.

C. Excitation and Trimming

An excitation frequency of $16\,\mathrm{kHz}$ was selected as the piezo sensor shows a good response around this frequency. This is likely due to a mechanical resonance of the two core halves. The bandwidth of this resonance proved to be high enough to enable successful operation of the system. A peak excitation flux density of $\approx 250\,\mathrm{mT}$ was selected which is well below the material's saturation flux density of $1.56\,\mathrm{T}$.

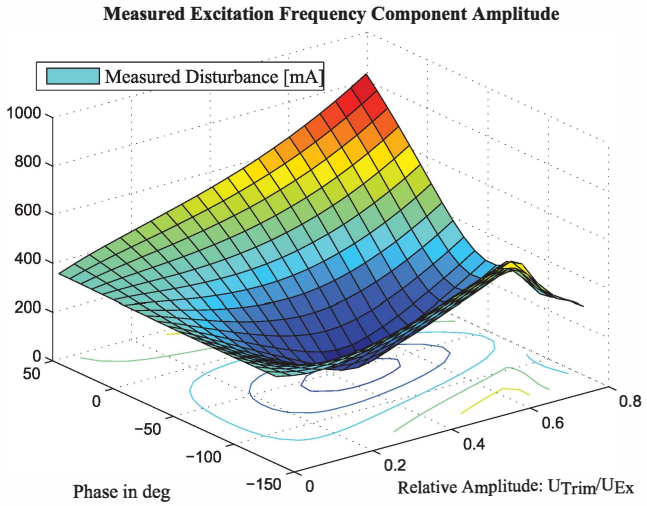

Fig. 10: Excitation frequency disturbance in the burden resistor as function of trimming voltage.

Using a higher excitation flux density would yield a higher output signal from the piezo sensor at the cost of increased core losses and power consumption.
A measurement from the prototype showing the measured excitation frequency component in the output signal as a function of trimming current phase and amplitude is given in **Fig. 10**. In the prototype, the trimming current source is implemented as a voltage source with a defined series impedance. Note that there is, as expected, a single point where the excitation signal vanishes from the burden winding. This point is found and selected by the algorithm described above. The bend in the plot results from an unstable amplifier which was not designed for operation with high relative trimming voltage.

D. Signal Processing

A digital signal processor handles the signal generation, demodulation, flux control, measurement routines and trimming. The two filters shown in **Fig. 4** are implemented as digital filters. The band-pass is a 10th order Chebyshev Type 2 filter with a passband of 11 kHz . . . 21 kHz providing 50 dB attenuation for frequencies below 7 kHz and above 33 kHz. The low-pass is a 4th order Chebyshev Type 2 filter with 1 dB attenuation at 10 kHz and 50 dB attenuation above 32 kHz. A standard PI controller is used as flux controller.

TABLE I: Measured transformer parameters.

Parameter	T1	T2
Turns Measurement Winding	1	1
Turns Burden Winding	20	20
Turns Excitation Winding	9	9
$L_{\mathrm{Measurement}}[\mu\ \mathrm{H}]$	0.77	0.78
$L_{\mathrm{Burden}}[\mu\ \mathrm{H}]$	297	302.8
$L_{\mathrm{Excitation}}[\mu\ \mathrm{H}]$	64.6	64.3
$k_{\mathrm{Measurement-Burden}}$	0.855 - 0.92	0.858 - 0.914
$k_{\mathrm{Measurement-Excitation}}$	0.83 - 0.92	0.849 - 0.927
$k_{\mathrm{Burden-Excitation}}$	0.924	0.927

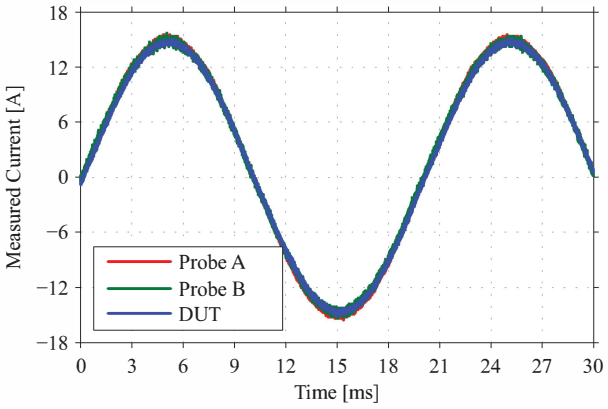

Fig. 11: Experimental measurement of an 8A, 50Hz sine signal utilizing the proposed magnetostriction-based current sensor.

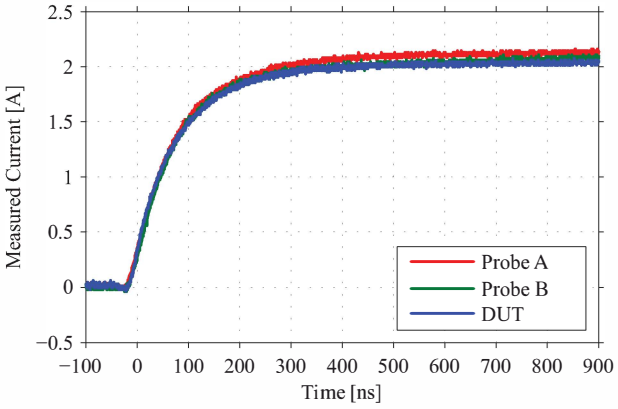

Fig. 12: Response to a 2 A current step. This test shows the fast dynamic performance of the sensor (note the timescale).

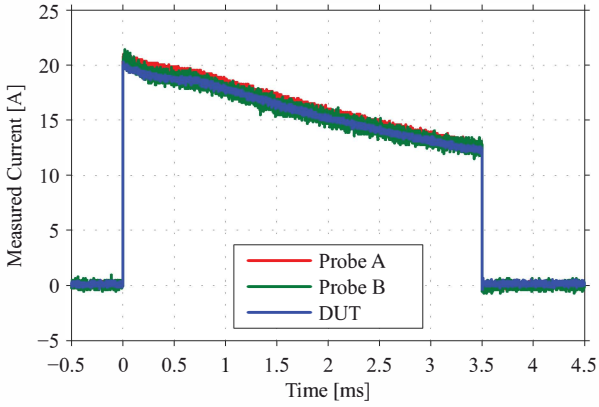

Fig. 13: Response to a 20 A current step. During this test, both the flux measurement concept and the current transformer are utilized. During the initial step, the current transformer is active whereas during the decaying current ramp the flux sensor is utilized to measure the signal.

E. Performance

The prototype has been compared to commercially available current probes. **Fig. 11** shows the measurement of a

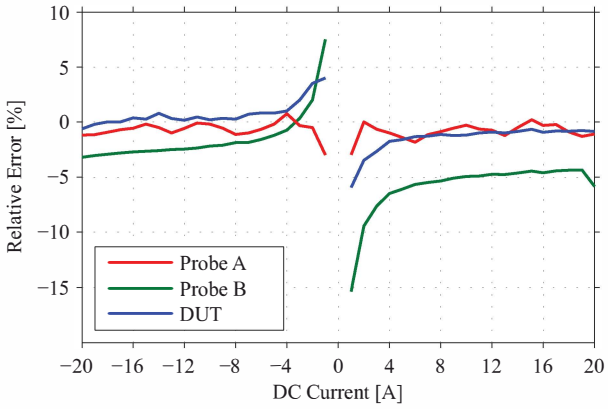

Fig. 14: Comparison of relative measurement errors with other common current probes.

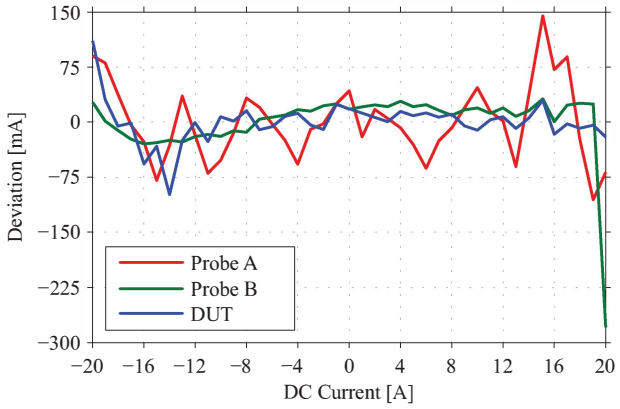

Fig. 15: Deviation of the measurement from its linear best first order fit for different current values and different current sensor manufacturers.

50 Hz, 8 A sine current. *DUT* denotes the magnetostriction based prototype. Note that 50 Hz is well below the lower cut-off frequency of the current transformer, thus, this signal is measured using the magnetostriction based compensation system only.

Fig. 12 depicts the response to a quickly rising 2 A current step. This plot solely shows the high-frequency response of the current probe, the dynamics are too fast for the magnetostriction system to take action. Thus, this response was generated by the current transformer only.

In **Fig. 13**, the step response to a much longer 20 A current step is shown. In this plot, the timescale is long enough that both, the current transformer and the flux compensation circuit, are involved in the current measurement.

Additionally, **Fig. 14** shows the relative measurement errors of the three current probes for DC-currents from −20 A to 20 A. A *Yokogawa WT3000* precision power analyzer, with an maximum error of ±2 mA over the full range, has been used as reference. The same data has been used to derive the linearity properties of all three probes. Least squares regression has been used to determine the best-fit line for each probe. **Fig. 15** shows the difference between the measured current and the best-fit lines of the probes. The best-fit integral nonlinearity (INL), defined as the maximum deviation between measured value and best-fit line, is given in **Table II**.

TABLE II: Linearity measurement results.

Probe	Best-Fit INL	Gain Error	Offset
Current Probe A	145 mA	−0.74 %	−2 mA
Current Probe B	279 mA	−3.77 %	−138 mA
DUT	126 mA	−0.41 %	−68 mA

F. Implementation Challenges

The successful implementation of a prototype proves the feasibility of this new flux sensing technique. However, several aspects require careful attention in order to ensure reliable and stable operation. First of all, the principle is based on magnetostriction, and hence a measurement of mechanical strain. It is therefore important to isolate the strain sensor from other mechanical influences, such as vibrations, that might generate erroneous sensor signals. Additionally, it is important that the sensor is immune to electromagnetic interference from the measuring signal and the excitation winding. This requires careful electric as well as magnetic shielding of the strain sensor. Furthermore, a solid magnetic core having no gap is preferable since it eliminates mechanical vibrations that might arise from the contacting core halves.

IV. Concept Extensions

Since there is no necessity for an air gap in the magnetic core, this technique of magnetic flux measurement can be utilized in other applications such as DC flux measurement in power distribution transformers or isolated DC-DC converters. As described in [14], isolated DC-DC converters may require some form of transformer core flux measurement in order to prevent core saturation. The technique described in this paper might be used to accomplish this. As the transformer is already excited by the DC-DC converter, no additional excitation winding is needed. This means that only a piezo sensor, measuring the core's magnetostriction, and analog amplification is required. As presented in the previous sections, the main part of the signal processing can be done digitally and thus requires no additional components in a digitally controlled converter.

V. Summary

A new and magnetic flux sensing principle has been proven in the application of a DC + AC current probe. This principle is based on measuring the changes in length of a magnetic component during its operation due the magnetostriction phenomenon. In order to detect these length changes, a piezo-electric transducer was adhered to the surface of a magnetic core. In addition, an AC signal was injected through an external winding in order to shift the input current's spectrum to higher levels, thus enabling the utilization of the piezo sensor.

By implementing a feedback loop comprising the piezo-electric sensor and the appropriate analog and digital circuitry, an accurate measurement of the input current in the

low frequency spectrum (including DC) was achieved. The combination of this magnetic flux measurement and the typically high bandwidth of a current transformer allowed to realize a current sensor able to measure currents up to 20 A and with a bandwidth ranging from DC to 20 MHz.

REFERENCES

[1] W. F. Ray and C. R. Hewson, "High performance Rogowski current transducers," in *Proc. of the Industry Applications Conference*, Oct. 8-12, 2000, pp. 3083–3090 vol.5.

[2] F. Costa, E. Laboure, F. Forest and C. Gautier, "Wide bandwidth, large AC current probe for power electronics and EMI measurements," *IEEE Transactions on Industrial Electronics*, vol. 44, no. 4, pp. 502–511, August 1997.

[3] G. Laimer and J. W. Kolar, "Design and experimental analysis of a DC to 1 MHz closed loop magnetoresistive current sensor," in *Proc. of the Applied Power Electronics Conference and Exposition (APEC), Austin, Texas*, vol. 2, Mar. 6-10, 2005, pp. 1288–1292 Vol. 2.

[4] A. Papp and H. Harms, "Magnetooptical current transformer. 1: Principles," *Applied Optics*, vol. 19, no. 22, pp. 3729–3734, 1980.

[5] P. Ripka, "Review of Fluxgate Sensors," *Sensors and Actuators A: Physical*, vol. 33, no. 4, pp. 129–141, 1992.

[6] S. Ziegler, R. C. Woodward, H. H.-C. Iu, and L. J. Borle, "Current Sensing Techniques: A Review," *Sensors Journal, IEEE*, vol. 9, no. 4, pp. 354–376, Apr. 2009.

[7] C. M. Johnson and P. R. Palmer, "Current Measurement Using Compensated Coaxial Shunts," *Science, Measurement and Technology, IEE Proceedings*, vol. 141, no. 6, pp. 471–480, 1994.

[8] F. Koga, T. Tadatsu, J. Inoue and I. Sasada, "A New Type of Current Sensor Based on Inverse Magnetostriction for Large Current Detection," *IEEE Transactions on Magnetics*, vol. 45, no. 10, pp. 4506–4509, Oct. 2009.

[9] LEM, "Isolated Current and Voltage Transducers (3rd edition)," LEM Components, 8 Chemin des Aulx, CH-1228 Plan-les-Ouates, 2004, cH24101.

[10] J. R. Leehey, L. Kushner and W. S. Brown, "DC Current Transformer," in *Proc. 13th Annu. Power Electron. Spec. Conf., Cambridge, MA, USA*, Jun. 1982, pp. 438–444.

[11] T. Zhang, C. Jiang, H. Zhang and H. Xu, "Giant Magnetostrictive Actuators for Active Vibration Control," *Smart Materials and Structures*, vol. 13, no. 3, pp. 473–477, Jun. 2004.

[12] T. Hilgert, L. Vandevelde and J. Melkebeek, "Comparison of Magnetostriction Models for Use in Calculations of Vibrations in Magnetic Cores," *IEEE Transactions on Magnetics*, vol. 44, no. 6, pp. 874–877, 2008.

[13] Y. Ishihara, H. Maeda, K. Harada and T. Todaka, "Performance of the Magnetostriction of a Silicon Steel Sheet with a Bias Field," *Journal of Magnetism and Magnetic Materials*, vol. 160, pp. 149–150, Jul. 1996.

[14] G. Ortiz, J. Mühlethaler and J. W. Kolar, "Magnetic Ear - Based Balancing of Magnetic Flux in High-Power Medium-Frequency Dual-Active-Bridge converter Transformer-Cores," in *Proc. of the 8th International Conference on Power Electronics (ECCE), Jeju, Korea*, May 30 - June 3 2011, pp. 1307–1314.